**SME Annual Meeting**
**Feb. 25 - 28, 2018, Minneapolis, MN**

# Preprint 18-018

## DEVELOPMENT OF A COMPREHENSIVE PILLAR AND ROOF MONITORING SYSTEM AT A STEEPLY DIPPING UNDERGROUND LIMESTONE MINE

**M. Murphy**, NIOSH, Pittsburgh, PA
**B. Slaker**, NIOSH, Pittsburgh, PA
**A. Iannacchione**, Univ. of Pittsburgh, Pittsburgh, PA
**G. Rashed**, NIOSH, Pittsburgh, PA
**M. Van Dyke**, NIOSH, Pittsburgh, PA
**G. Buchan**, NIOSH, Pittsburgh, PA
**T. Minoski**, NIOSH, Pittsburgh, PA
**D. McElhinney**, NIOSH, Pittsburgh, PA
**J. Winfield**, Graymont PA Inc., Pleasant Gap, PA

### ABSTRACT

The National Institute for Occupational Safety and Health (NIOSH) has previously established pillar design guidelines for the underground stone mining industry. These guidelines were created from an empirical database of pillar observations and were largely drawn from shallow, flat-lying mining operations. Current trends forecast a great amount of underground stone mines developing under deeper cover, higher seam dips, and more frequent multiple-seam mining configurations than in the past. The complex loading conditions and limited experience in these environments presents a substantial increased risk of ground failure. To investigate these loading conditions, NIOSH has installed a pillar and roof monitoring system at an underground limestone mine in central Pennsylvania. The mine is operating in a seam with dips ranging from 13 to 18 degrees and overburdens ranging from 275 m (900 ft) to 425 m (1,400 ft). Instrumentation installed in an undeveloped pillar and in surrounding strata is currently measuring pillar and roof behavior in response to stress redistribution during excavation. Laser scans are being used to measure ground displacement and changes in conditions associated with local mining conditions and significant geological features. Initial stress measurements show a gradual increase in stress in response to mining, and stress changes that correspond with blasts. The seismic system is operational, with calibration events signaling on each of the 18 sensors.

### INTRODUCTION

Improving mine-wide ground control stability can help reduce the potential for catastrophic failure of underground structures. The National Institute for Occupational Safety and Health (NIOSH) has conducted prior research in stone pillar design and has established fundamental pillar design guidelines for the underground stone mining industry, which resulted in the development of the S-Pillar program (Esterhuizen et al., 2011; Esterhuizen and Murphy, 2015). The data that constitute the S-Pillar program were derived from past mining experience that was almost exclusively drawn from shallow, flat-lying, single-level mining operations[1]. Stakeholder interactions with NIOSH researchers have indicated that increased numbers of underground stone operations are expected to mine under significantly deeper cover, with greater seam dips, and under multi-level operating conditions (Slaker and Murphy, 2016). The complex loading conditions and limited experience in these challenging environments present a substantial increased risk of ground failure. Inadequate pillar design in these new and challenging environments could result in catastrophic wide-area pillar collapses and an increased safety burden to miners working in the U.S. limestone mining industry. To develop design guidelines and prevent inadequate pillar designs for these challenging environments, NIOSH is currently conducting detailed pillar response investigations at case-study mine sites operating in challenging environments.

The current case study documents the pillar response to excavation in a deep and steeply dipping limestone mine located in central Pennsylvania. Uniaxial accelerometers and biaxial stressmeters are installed in the ribs of a development entry. An adjacent development entry and crosscuts will be mined to outline the study pillar sometime in the next two years. The plan is to measure pillar and strata behavior in response to loading and stress redistribution during the outlining of the pillar. Additionally, routine laser scans are made to monitor roof, floor, and rib displacement associated with local mining conditions and significant geological features. To the knowledge of the authors, this is the first time the development of a stone pillars has been monitored in this way.

This project is a cooperative effort between NIOSH and the operator of the mine. NIOSH provided the data acquisition and monitoring instrumentation. The mine operator provided access to the underground workings and the underground power grid, as well as conducting the drilling of sensor boreholes and maintaining the instrumentation array. This paper gives a detailed overview as well as preliminary results from the displacement monitoring, geotechnical measurements, numerical modeling calibration, stress monitoring, and seismic system.

### SITE DESCRIPTION

The case study is at the Pleasant Gap mine, an underground room-and-pillar limestone mine owned by Graymont PA Inc. and located in central Pennsylvania. In the past, NIOSH and the operator had jointly installed a surface-based, mine-wide microseismic monitoring system to evaluate the relationship between microseismicity and roof instability (Bajpayee et al., 2008). The current study is unique in that a seismic system is being used to study more precisely the relationship between mine development and stone pillar loading in a deep, steeply dipping environment.

A map of the Pleasant Gap mine is shown in Figure 1. The limestone seam dips approximately 13 to 18 degrees in the southeast direction. The mine is located within a structurally complex area of tightly folded anticlines and synclines. The study area, highlighted in Figure 1, is within one of the deepest parts of the mine and is approaching 425 m (1,400 ft) in overburden. Data made available by the mine indicated that the horizontal stress conditions have been measured at two different locations, using the U.S. Bureau of Mines (USBM) Borehole Deformation Gauge, in 2009 and 2014. The 2009 test measured the maximum horizontal stress direction to be N48°E

[1] For the S-Pillar software dataset, shallow is defined as less than 305 m (1,000 ft) and flat-lying is defined as less than a 5-degree dip (Esterhuizen and Murphy, 2015).

with a stress magnitude ranging from 20–31 MPa (3,000–4,600 psi). The 2014 test measured an orientation of N50°E with a magnitude of 32 MPa (4,649 psi). The regional stress field is reported to be N60°E (Rones, 1969).

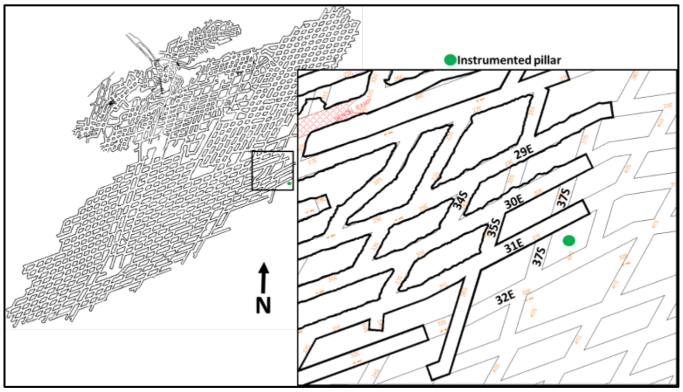


**Figure 1.** Map of the Pleasant Gap mine, including a detailed view of the instrumented area for the case study.

The mine operates in the Valentine Formation, which is typically light grey, extremely fine-grained limestone, and approximately 21.3-m (70-ft) thick. The overlying Centre Hall Formation contains approximately 9.1-m (30-ft) of medium-dark-gray limestone. During mine development, the roof horizon begins at the parting between the Valentine and Centre Hall formations. Within the overlying Centre Hall Formation, horizontal Bentonite clay bands are particularly significant as they can be conduits of water and extend great distances (Rones, 1969). Below the Valentine Formation is the Valley View limestone member of the Linden Hall Formation. It is typically dark-gray and averages 12.8-m (42-ft) thick.

The rib of the instrumented pillar is in the 31E development entry (Figure 2). The advancement of the 37S and 40S crosscuts and 32E advancement development entry will outline the instrumented pillar. The underground mine design incorporates a variety of pillar sizes, but the planned dimensions of the instrumented pillar and adjacent crosscut width is shown in Figure 2. The 31E development entry width and mining height, measured by a Maptek I-Site 8200 laser scanner, is shown in Figure 3.

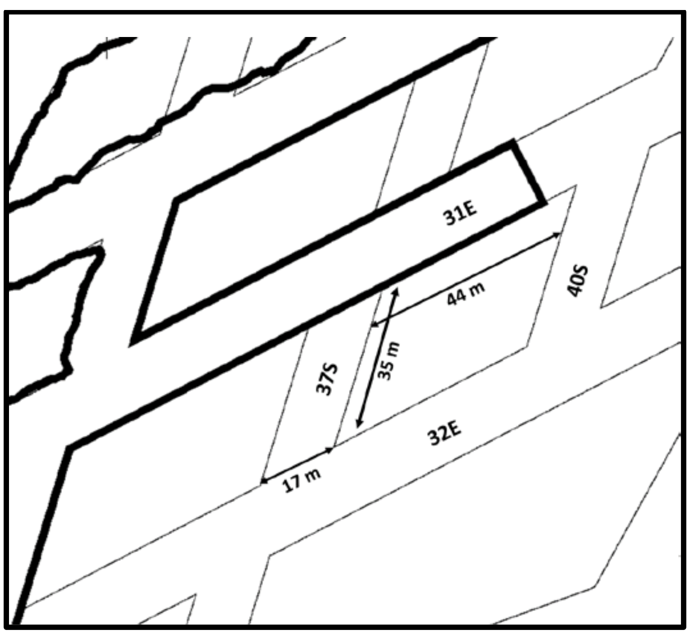


**Figure 2.** Planned dimensions of the instrumented pillar and crosscut.

Two prominent fracture patterns, referred to as the J1 and J2 joints by the operator, are found throughout the mine. J1 joints are sub-parallel to the direction of maximum horizontal stress and are roughly parallel to the strike of the strata. J2 joints are generally perpendicular to the direction of maximum horizontal stress. J1 joints are sometimes open, especially at shallow overburden. Both J1 and J2 joints are often calcite filled. Joints other than the J1 and J2 occur in irregular patterns throughout the mine. Bedding planes often containing thin bentonite clay bands are found most often in the roof and floor strata. In isolated bench locations prominent bentonite clay bands have been associated with rib instabilities.


**Figure 3.** Entry width and mining height adjacent to the instrumented pillar.

The J1 and J2 joints were identified near the mining faces in development entries 31E, 30E, and 29E. Cutters, containing shear failure often associated with excessive levels of horizontal stress, are present within the study area and are most often found in the crosscuts and to a lesser degree along either side of mine headings (parallel to strata strike). Roof instabilities increase when J1 and J2 joints intersect and can create roof cavities 0.9-1.2 m ft (3-4 ft) deep, exposing the weaker Centre Hall Formation.

## DISPLACEMENT MONITORING AND GEOTECHNICAL MEASUREMENTS

The Maptek I-Site 8200 laser scanner was used to obtain mine geometry, monitor strata displacements, and map geological features around the study area. Laser scan surveys were conducted on May 17–18, 2017 to create a baseline of the mine geometry, shown in Figure 4, and overlain on the projected mine development. The point cloud for the mine geometry was created from 21 separate laser scans, represented by yellow squares in Figure 4. Also shown in the figure are the locations for the biaxial stressmeters and seismic sensors, which will be discussed in more detail in subsequent sections.

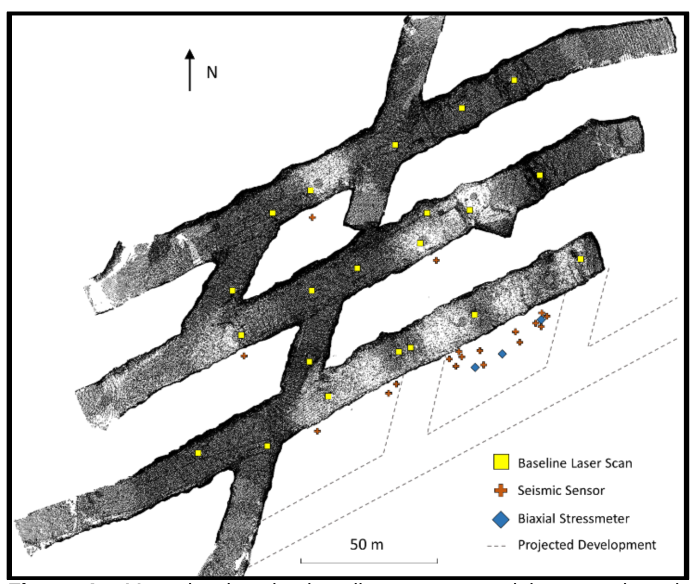


**Figure 4.** Map showing the baseline survey overlain on projected mine development with sensor locations highlighted.

The laser scanner and the Geotechnical Tools within the Maptek I-Site software (Maptek, 2017) were used to map the J1 and J2 joint sets, bedding features, prominent fracture planes, and the mine orientation. These features are shown in Figure 5. Strikes and dips were measured in the field with a Brunton Compass. J1 joints were oriented N61°E and averaged 4.6 m (15 ft) apart from each adjacent J1. The J2 joints were more variable than the J1 joints and could vary between 0.15 m (0.5 ft) to 1.5 m (5 ft) in spacing and the strike averaged N19°W. The bedding of the Valentine formation was measured to be N55°E and dip 18°SE.

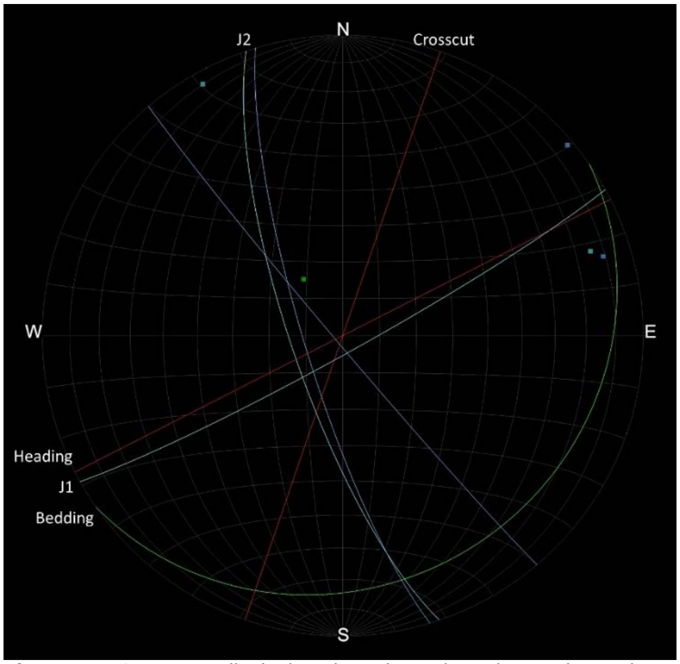


**Figure 5.** Stereonet displaying the mine orientation and prominent discontinuities.

As the 32E, 37S, and 40S advancement occurs, future laser scan surveys will be compared to the baseline to monitor displacement and spalling that occurred in response to loading. Significant geologic feature changes will also be monitored to investigate their potential role in unstable roof formation.

## FLAC3D NUMERICAL MODELING

Due to the complex geometry inside of the mine, the developed pillars have a rhombus shape (Figure 2 and Figure 4). It is unknown if the vertical stress distribution inside of the study pillar would be concentrated differently than that of a square pillar in a flat-lying deposit. An elastic FLAC3D (Itasca, 2012) numerical model was created to further understand the vertical stress distribution of a rhombus-shaped pillar in a dipping seam. The numerical model represents the mine geometry around two fully developed pillars north of the instrumented pillar. The workflow for the model generation was initiated from the baseline laser scanning survey (Figure 4). From the baseline survey point cloud, coordinates were picked from the scan and imported into Rhino 5 (Rhinoceros, 2017) to create the geometry of two fully developed pillars, entries, and crosscuts. The geometry created in Rhino 5 was inserted into the Griddle software (Itasca, 2016) to create the FLAC3D grid, shown in Figure 6.

The dimensions of the Griddle-generated FLAC3D model were 312 x 275 x 211 m (1,023 x 902 x 692 ft). The outer boundaries of the model were fixed against normal displacement, while allowing displacement to take place along the boundary surface (roller boundaries). The entry, crosscut, and pillar dimensions measured from the laser scans and implemented in the model are similar to those found in Figure 2 and Figure 3. The laser scans were able to capture the apparent dips of the seam in the study area, 17° and 4°, which were also represented in the model (Figure 6). In the numerical model, it was assumed that the immediate roof and the immediate floor have the same apparent dips as the mining horizon. The element size of the pillars was approximately 0.5 m (1.6 ft). Table 1 summarizes the elastic constants for the limestone, roof, and floor strata used in the model (Zipf, 2006).

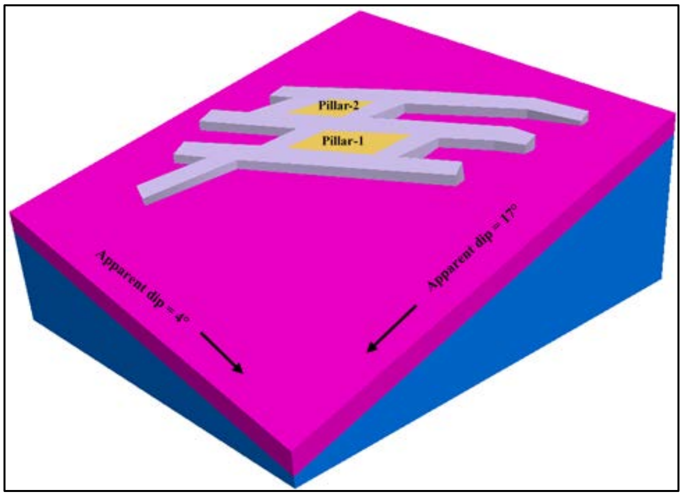


**Figure 6.** Representative pillar model created in FLAC3D.

**Table 1.** Rock material input parameters (after Zipf, 2006).

| Rock Type | Young's modulus (GPa) | Poisson's ratio |
|---|---|---|
| Light gray limestone Valentine (pillar and immediate floor) | 20 | 0.25 |
| Dark gray limestone Valley View (floor) | 15 | 0.25 |
| Dark gray limestone Centre Hall (immediate roof) | 15 | 0.25 |
| Sandstone (Main roof) | 12 | 0.25 |

The model was solved in two steps corresponding to the pre-mining and development stages. To reduce complexity and model run time, only the first 133 m (400 ft) of the overburden above the roof horizon was modeled, and a pressure equivalent was applied to the top surface to represent the remaining 274 m (900 ft). The maximum and minimum horizontal stresses at the mine level were initialized to 30.0 MPa (4,350 psi) and 16.0 MPa (2,320 psi). The high horizontal stress was aligned parallel to the length of the pillar. During the pre-mining stage, the initial stresses and the boundary conditions were applied and solved to equilibrium. The resulting pre-mining vertical stress at the mine level was roughly 9.9 MPa (1,435 psi) after the model came to equilibrium, which is in the expected range for that depth (Hoek and Brown, 1980).

In the development stage, the elements corresponding to entries and the crosscuts were removed, and the model was again solved to reach equilibrium. The resulting variation of the vertical stress in Pillar-1 is shown in Figure 7, while Figure 8 and Figure 9 show the variation of the vertical stresses at cross-sections A-A and B-B, respectively. Cross-section A-A was taken at the mid-height of the pillar, parallel to the pillar's top surface, and cross-section B-B was taken at the mid-length of the pillar. Due to the apparent dips of the limestone seam, the vertical stress distribution is not uniform in the pillar. Figure 7 shows that the shorter entry height side of the pillar is subjected to more vertical stress than the tall side, possibly because the stiffness of the short side of the pillar is higher than that for the tall side. For the same amount of roof displacement, the short side will take more load than the tall side.

Based on these modeling results, it is expected that the short side of the pillar will show higher stress and will be an area of interest when analyzing the seismic data. NIOSH researchers will continue to improve the modeling accuracy as the instrumentation data becomes available during the 32E, 37S, and 40S advancement. Future modeling is expected to include yielding analysis to investigate failure zones within the modeled pillar compared to seismic event locations.

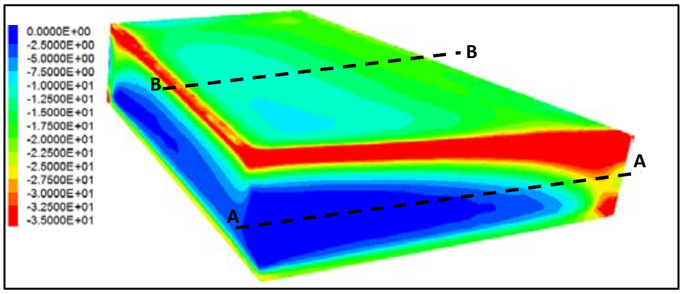


**Figure 7.** Vertical stress distribution in Pillar-1 (scale in MPa).

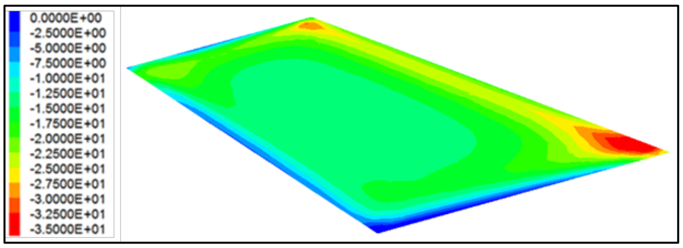


**Figure 8.** Vertical stress distribution at cross-section A-A (scale in MPa).

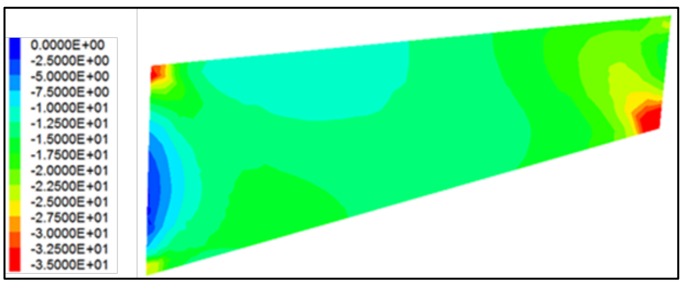


**Figure 9.** Vertical stress distribution at cross-section B-B (scale in MPa).

## STRESS MONITORING

Vibrating wire biaxial stressmeters (Geokon, 2017) were installed in the instrumented pillar to determine relative stress changes as advancement occurs. NIOSH researchers have had success in the past with using biaxial stressmeters to measure long-term pillar loading in room-and-pillar hard rock mines as mining advanced. In a past study, vibrating wire stressmeters were used to precisely and reliably monitor long-term stress changes in a backfilled section of a large-opening room-and-pillar mine over 16 years (Tesarik et al., 2009).

Figure 4 and Figure 10 show the locations of three biaxial stressmeters, indicated by blue diamonds and notated as VW1, VW2, and VW3. These locations were determined by the numerical models shown in the previous section. The most inby biaxial stressmeter, VW1 (Figure 4 and Figure 10), was not installed as deep into the pillar, capturing the most highly stressed accessible region of the pillar. VW2 and VW3 are approximately 9.5 m (31 ft) from the open rib, and VW1 is approximately 4.5 m (15 ft) from the open rib. All sensors are fully grouted and oriented with one of the two axes aligned nearly vertical.

Biaxial stressmeter data were collected for a period of 51 days, beginning of June 21st, 2017. The stress readings represent a change in stress from July 1st, 11 days after data collection began, to allow time for the grout to cure. The stress displayed is the major principal stress, which is initially assumed to be vertical. Many blasts occurred throughout the mine during the monitoring period, but Blast Locations A and B (Figure 10) are the only areas of development within approximately 250 m (820 ft). The recorded stress on the three sensors and the date of each blast during the monitoring period are labeled in Figure 11.

Each blast resulted in a linear face advance of 3.3–5.2 m (11–17 ft), unless marked as "Trim", which are blasts that minimally affect the natural rock support and are intended to shape the heading into the approximate planned dimension. The full blasts all had an immediate pronounced effect on the stressmeters, while the trim blasts appear to have caused no changes in the pillar stress. All three stressmeters are also showing a gradual increase in stress. While the immediate effect of a blast on the stress field cannot be precisely predicted, a trend of increasing pillar stress with development nearby is expected. The stress field will continue to be monitored as the adjacent entry (32E) and two crosscuts (37S and 40S) are mined to form the pillar. The stress redistribution data, measured as the pillar is formed, will be used to improve the accuracy of the FLAC3D numerical model.

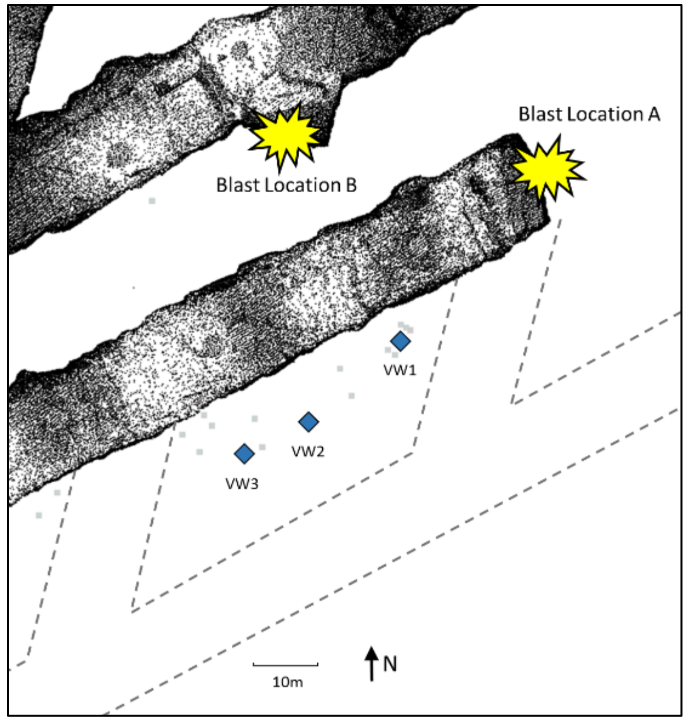


**Figure 10.** Locations of biaxial stressmeters and nearby blasts.

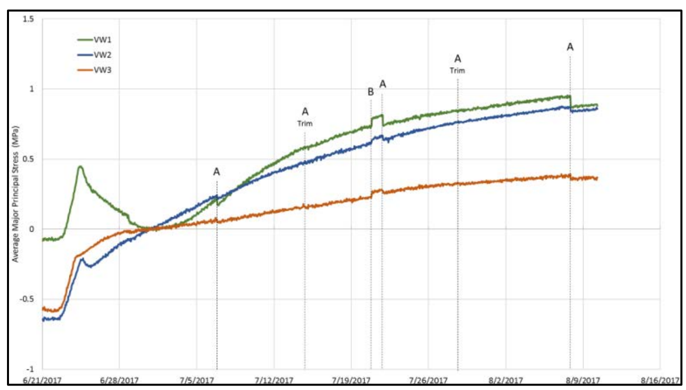


**Figure 11.** Maximum principal stress over time as recorded from the three biaxial stressmeters, with nearby blasts marked.

## SEISMIC MONITORING SYSTEM

Seismic events are a common and expected response to a moving rock mass as stresses are redistributed and fractures are produced due to development loading (Iannacchione et al., 2004; Simser et al., 2015). If the fractures that develop due to loading near a pillar can be captured and analyzed, inferences about the state of stress within the pillar and the extent of damaged zones can be made. Uniaxial accelerometers, coupled with the ESG Portable Paladin® Data Acquisition Unit (ESG Solutions, 2017), were installed at varying depths into the instrumented pillar and surrounding area to capture seismic event frequency and locations in response to loading. The sensors have a frequency response of 50 Hz to 5 kHz. Figure 4 and

Figure 12 show the locations of the eighteen sensors installed around the study area.

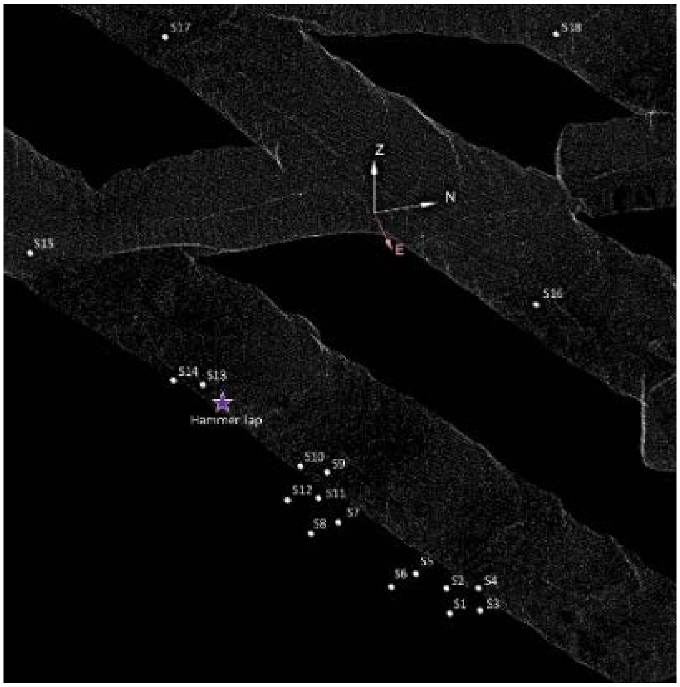


**Figure 12.** Hammer tap location and seismic sensor locations.

Sensors 1 through 14 were fully grouted into seven separate 9.5–10 m (31–33 ft) holes, with one sensor installed at the end of the hole and the other was positioned halfway through. Each of the holes were slightly sub-horizontal and at a collar height of 1.2 m (4 ft) or 5.5 m (18 ft) to vary the sensor locations as much as possible to improve seismic event location. Figure 13 shows a detailed view of the Sensor 1 through 14 locations inside of the planned development. The depth of the sensor locations was limited to accurately locate the end of the hole after drilling. Hole depths exceeding roughly 10 m (33 ft) would require additional drill steel and increase the likelihood of drift during drilling. Confidence in the drill hole survey accuracy was required for the researchers to locate low-magnitude rock fracture events with high precision.

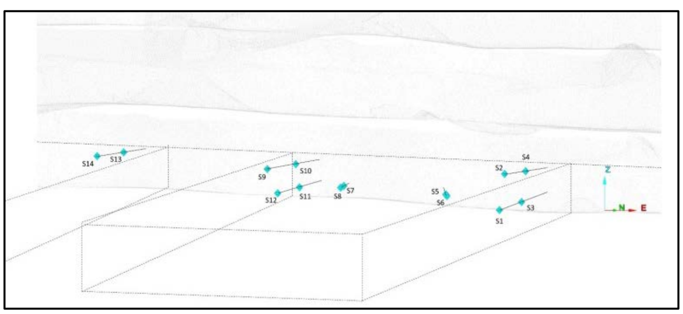

Figure 13. Detailed view of Sensor 1-14 locations.

Sensors 15 through 18 were installed at the end of 4.6-m (15-ft) holes, angled approximately 45 degrees into the roof, over the pillar, and affixed to the end of the hole by epoxy. These sensors are not clustered near the study pillar, but rather are located in the surrounding area to help resolve other ground responses that may correspond with pillar loading. Each sensor is wired back to the ESG Portable Paladin Data Acquisition Unit.

Due to concerns with cable management around the blast, the only data collected to date has been calibration events produced with a rock hammer on a survey point with a known location. Figure 12 shows the location of one of the calibration hammer taps (indicated by a purple star), while Figure 14 shows the corresponding waveform detected on each of the sensors.

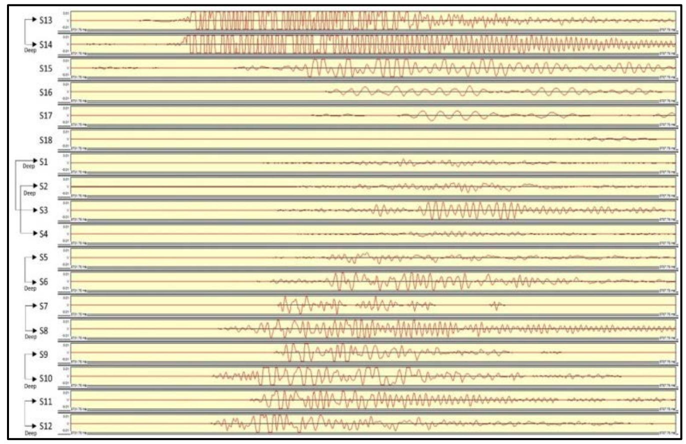


Figure 14. Seismic signal recorded on all 18 sensors from a hammer tap at the survey point. Arrows indicate shared holes.

Varying amounts of noise are present in the signals which may obscure low magnitude events in the waveforms. Efforts to improve sensor calibration and filtering are ongoing. Development blasts around the study area with known source locations will be used to evaluate source location accuracy. A detailed velocity model and event location algorithms are being explored.

Seismic events inside of the pillar will be analyzed as the adjacent entry (32E) and two crosscuts (37S and 40S) are mined to form the pillar. The analysis will be used to calibrate a yielding FLAC3D model. Seismic events in the strata, in response to mining, will be analyzed to investigate cutter development and the J1 and J2 joint response.

## CONCLUSIONS

Stakeholder interactions with NIOSH researchers have indicated that large-opening room-and-pillar mines are expected to operate under much deeper cover with greater seam dips. The complex loading conditions and limited experience in these challenging environments presents a substantial increased risk of ground failure. NIOSH is currently conducting detailed pillar response investigations at case-study mine sites operating in challenging environments. These investigations involve developing and installing a comprehensive pillar and roof monitoring system.

For the current study, a monitoring system has been installed in a deep and steeply dipping limestone mine in central Pennsylvania. The study will document pillar loading response and strata behavior as a currently exposed rib is developed into a full pillar. Pillar and strata behavior, along with significant geologic feature changes, in response to loading and stress redistribution, will be monitored for two years using uniaxial accelerometers, stressmeters, and laser scans.

The preliminary data presented in this paper outline the strategy for continuing the study until the pillar is fully developed. Future laser scans will be compared to the baseline scan to monitor roof, rib, and floor displacement. The stressmeter data already presented has shown minor vertical stress changes inside of the undeveloped pillar in response to nearby blasting. Uniaxial accelerometers have been installed throughout the study area. Preliminary calibration of the seismic system has been successful with hammer taps at known survey points throughout the study area. Future seismic data will investigate the state of stress within the pillar and the extent of any damage in the pillar or surrounding roof. An elastic FLAC3D numerical model was developed to find the expected areas of high stress inside of a pillar in a dipping seam. As additional displacement, stressmeter, and seismic data are obtained during the study pillar development, the numerical model will be improved to include yielding and calibrated to investigate pillar designs in deep and steeply dipping seams.

At the conclusion of this study, pillar design guidelines will be developed for this challenging condition to prevent catastrophic wide-area pillar collapses and an increased safety burden to miners working in the U.S.

## DISCLAIMER

The findings and conclusions in this report are those of the author(s) and do not necessarily represent the views of the National Institute for Occupational Safety and Health. Mention of any company or product does not constitute endorsement by NIOSH.

## REFERENCES

Bajpayee, T., Iannacchione, A.T., and Schilling, S.R., 2008, "Detecting strata fracturing and roof failures from a borehole based microseismic system," *Proceedings of the 27th International Conference on Ground Control in Mining*.

ESG Solutions (2017). Products – Paladin Data Acquisition, Sensors, Software. Retrieved from https://www.esgsolutions.com/mining-and-geotechnical/products

Esterhuizen, G S., Dolinar, D.R., Ellenberger, J.L., and Prosser, L.J., 2011, "Pillar and roof span design guidelines for underground stone mines." Pittsburgh, PA: U.S. Department of Health and Human Services, Public Health Service, Centers for Disease Control and Prevention, National Institute for Occupational Safety and Health, DHHS (NIOSH) Publication No. 2011-171, IC 9526, 2011 May; Retrieved from http://www.cdc.gov/niosh/mining/works/coversheet1355.html

Esterhuizen, G.S., and Murphy, M.M., 2015, "Mining Product: S-Pillar – Software for Stone Mine Pillar Design Version 1.02. Pittsburgh, PA: U.S. Department of Health and Human Services, Public Health Service, Centers for Disease Control and Prevention, National Institute for Occupational Safety and Health, 2011 Jan. Retrieved from https://www.cdc.gov/niosh/mining/works/coversheet1817.html

Geokon (2017). Biaxial Stressmeters (VW) Model 4350. Retrieved from http://www.geokon.com/4350.

Hoek, E., and Brown, E.T., 1980, "Underground Excavations in Rock," London: Institute of Mining and Metallurgy.

Iannacchione, A.T., Batchler, T., and Marshall, T.E., 2004, "Mapping hazards with microseismic technology to anticipate roof falls--a case study," *Proceedings of the 23rd International Conference on Ground Control in Mining*, pp. 327–333.

Itasca Consulting Group, Inc., 2012, FLAC3D – Fast Lagrangian Analysis of Continua in Three Dimensions, Ver. 5.0., Minneapolis: Itasca.

Itasca Consulting Group, Inc., 2016, Griddle, Version 1.0, Minneapolis: Itasca.

Maptek, 2017, I-Site Studio (computer software). Retrieved from http://www.maptek.com/products/i-site/i-site_studio.html

Rhinoceros (2017). Rhino3D (computer software). Retrieved from https://www.rhino3d.com/

Rones, M., 1969, "A lithostratigraphic, petrographic and chemical investigation of the Lower Middle Ordovician carbonate rocks in Central Pennsylvania." General Geology Report G 53, Bureau of Topographic and Geologic Society, Commonwealth of Pennsylvania.

Simser, B., Deredin, R., Jalbout, A., and Butler, T., 2015. "Use of microseismic monitoring data as an aid to rock mechanics decision making and mine design verification." *49th US Rock Mechanics/Geomechanics Symposium*, American Rock Mechanics Association.

Slaker, B.A., Murphy M.M., 2016, "Underground stone mine pillar design in challenging conditions," *The 21st Annual Underground Stone Safety Seminar*. Louisville, Kentucky, December 6-7.

Tesarik, D.R., Seymour, B.J., and Yanske, T., 2009, "Long-term stability of a backfilled room-and-pillar test section at the Buick Mine, Missouri, USA." *International Journal of Rock Mechanics and Mining Sciences*, Vol. 46, No. 7, pp. 1,182–1,196.

Zipf, Jr., R.K., 2006, "Numerical modeling procedures for practical coal mine design." *Proceedings of the 41st U.S. Rock Mechanics Symposium*, Golden, Colorado, June 17-21, 2006. Alexandria, VA: American Rock Mechanics Association, pp.1–11.